High-Power Microwave Generation by Excitation of a Plasma-Filled Rippled Boundary Resonator

YUVAL CARMEL, MEMBER, IEEE, K. MINAMI, WEIRAN LOU,
R. ALAN KEHS, SENIOR MEMBER, IEEE, WILLIAM W. DESTLER, MEMBER, IEEE,
VICTOR L. GRANATSTEIN, SENIOR MEMBER, IEEE, D. K. ABE, AND J. RODGERS

Abstract—**An experimental demonstration of a strong enhancement of the interaction efficiency in a high-power relativistic backward-wave oscillator when plasma is injected is presented. Controlled plasma injection enhances the interaction efficiency over the vacuum case by a factor of up to 8 to a value of about 40%. A linear theory of electromagnetic wave generation in plasma-loaded corrugated wall resonators is reviewed. A number of physical mechanisms are considered to account for the enhanced interaction, including two variations of a three-wave interaction involving the electron-beam slow space-charge wave, the slow electromagnetic waves in the structure, and the quasi-electrostatic waves in the plasma.**

I. INTRODUCTION

THE FIELD of plasma electronics dates back to 1949 when several authors [1] discussed the excitation of electromagnetic waves in a plasma by an electron beam by virtue of stimulated Čerenkov radiation. Since 1949 this field of research has expanded to include beam heating of plasmas, collective acceleration of charged particles by plasma fields, and the excitation and amplification of electromagnetic waves. This last area has been referred to in the literature as "plasma microwave electronics" [2].

The introduction of plasma into vacuum microwave devices can have several beneficial effects. It is expected that plasma microwave devices could be tuned in frequency by exercising control over the plasma density up to the millimeter wave regime. Finally, extremely high-power microwave devices may be realized by using beam currents well above the space-charge-limiting current in vacuum. These currents may be realized by using a plasma to neutralize the beam space charge.

The practical realization of plasma microwave devices involves serious difficulties which have yet to be fully overcome. These difficulties include the generation of uniform, steady-state, highly ionized plasmas, high noise levels which may have an adverse effect on the operation of microwave amplifiers depending on the application envisioned, the lack of a fully developed linear and nonlinear theory of plasma devices, and the problem of coupling the electromagnetic radiation both into and out of the plasma.

In particular, the problem of coupling the electromagnetic radiation to plasma waves has proved to be quite complicated and must be resolved before truly effective plasma microwave devices may be realized. The difficulty lies with the slow longitudinal oscillations which are excited in the plasma. For nonrelativistic beams, these oscillations have very slow phase velocities ($v_{phase} \ll c$) and behave like quasi-electrostatic oscillations. As a consequence, they are mostly trapped in the plasma. Recent efforts have sought to reduce the losses during the extraction of energy from a plasma by using relativistic electron beams. Under these conditions the wave excited in the plasma may have a phase velocity $v_{phase} \sim c$, allowing it to be more easily extracted from the plasma.

The purpose of this work is to study the feasibility of generating very high-power microwave radiation by using relativistic electron beams in plasma-loaded microwave devices. Over the years a wide variety of high-power microwave (HPM) vacuum devices have been studied, including the well-known magnetron, klystron, and backward wave oscillator, as well as newer devices such as the gyrotron, the free-electron laser, and the virtual cathode oscillator [3]. All of these sources have one thing in common—they are driven by an intense unneutralized electron beam which interacts unstably in high vacuum with an electromagnetic wave, leading to the conversion of the kinetic energy of the beam into electromagnetic radiation. The power levels available from such devices have grown by an order of magnitude every decade since 1940. For example, advanced, large diameter, overmoded backward wave oscillators (like the multiwave Čerenkov and multiwave diffraction generator) have recently achieved efficient operation at power levels of about 15 GW [4] at a wavelength of 3 cm and 4.5 GW [5] at a wavelength of 6.5 mm, and operation at a wavelength of 2 mm has been demonstrated [6]. The thrust of this work is to evaluate efficiency enhancement in a small diameter, relativistic backward-wave oscillator using a different approach—that of plasma loading.

Manuscript received October 24, 1989; revised January 22, 1990. This work was partially supported by the Strategic Defense Initiative Organization and the Air Force Weapons Laboratory through contracts administered by Harry Diamond Laboratories and the Naval Research Laboratory, respectively.

Y. Carmel, W. R. Lou, W. W. Destler, V. L. Granatstein, D. K. Abe, and J. Rodgers are with the Laboratory for Plasma Research, Energy Research Building, University of Maryland, College Park, MD 20742.

K. Minami is with Niigata University, Niigata City, Japan.

R. A. Kehs is with Harry Diamond Laboratories, Branch 22900, 2800 Powder Mill Road, Adelphi, MD 20783.

IEEE Log Number 9035687.

0093-3813/90/0600-0497$01.00 © 1990 IEEE

Backward-wave oscillators (BWO's) are ideal candidates for the evaluation of plasma effects on microwave generation because they are relatively simple devices, providing fairly effective conversion of electron-beam energy into radiation, and can be easily filled with plasma. Initial studies [7], [8] have utilized background plasmas produced by the electron-beam impact ionization of a low-pressure neutral gas background and have demonstrated enhanced microwave output power. In recent experiments high-power microwave radiation was observed in a relativistic backward-wave oscillator which was externally filled with a highly ionized plasma [9]. Controlled plasma injection enhanced the interaction efficiency relative to the vacuum case by as much as a factor of 8, resulting in an efficiency of about 40%.

Section II of this paper reviews wave propagation in a plasma-filled smooth-walled waveguide; Section III contains a discussion of the space-charge-limiting current in plasma-loaded waveguides. A linear theory of plasma-filled corrugated structures is reviewed in Section IV. Section V summarizes the results from an experimental, plasma-loaded, high-power BWO that demonstrated a strong enhancement in the interaction efficiency, and Section VI contains a discussion of the results, including such questions as possible coupling mechanisms, mode stability, and future trends in plasma microwave electronics.

II. Review of Wave Propagation in Plasma-Filled, Smooth-Walled, Cylindrical Waveguides

Plasma effects in conventional microwave-generating devices can usually be neglected since the plasma frequency of the background gas is much smaller than the plasma frequency of the electron beam. Typically, $\omega_p/\omega_b < 10^{-2}$, where $\omega_p = (eN_p/m_e\epsilon_0)^{1/2}$ is the background plasma frequency, and $\omega_b = (eN_b/m_e\epsilon_0)^{1/2}$ is the beam-plasma frequency. Recent theoretical studies, however, have predicted that the presence of a plasma in high-power microwave devices may lead to enhanced performance, attracting renewed scientific interest [2], [10]–[16].

One of the characteristics of a fully ionized plasma is its ability to support electric fields of almost arbitrarily large amplitude. A small local deviation from neutrality in an otherwise neutral plasma can give rise to very large local fields. As an example, consider a uniform plasma with an average density of 10^{14} cm^{-3}. A 1% fluctuation in the local electron density over a distance of 1 mm produces a local electric field of $\sim 10^6$ V/cm. This capability of sustaining very high electric fields makes plasma attractive for use in high-power density microwave generators.

The presence of a plasma in a waveguide changes the characteristics of the guide and adds new slow modes of propagation. For the purpose of this discussion, the term "plasma" will be used to describe a fully ionized gas which, in the absence of external disturbances, is electrically neutral. It is further assumed that the ions in the plasma are stationary, and that the electrons have no thermal or random velocities and undergo no collisions. In other words, we will consider an ideal electron plasma. The term "plasmaguide mode" will be used to denote any of the additional waveguide modes that exist due to the presence of the plasma inside of the guide. These are the slow-wave modes on a nondrifting, ion-neutralized plasma column [17].

In order to generate microwave radiation, we are interested in waves that can cause bunching in an axially streaming relativistic electron beam. Therefore only waves with axial components E_z will be considered. There are two such families of waves: The first is the familiar $TM_{l\nu}$ family of electromagnetic modes which will be somewhat modified by the presence of the plasma, and the second is a family of plasmaguide modes.

As was demonstrated by Trivelpiece and Gould (T–G) [17], the dispersion relation for a plasma-loaded, smooth-walled, cylindrical waveguide immersed in an infinitely large axial magnetic field is given by:

$$\frac{\omega^2}{c^2} = k_z^2 + \frac{(p_{l\nu}/R_0)^2}{1 - \omega_p^2/\omega^2} \tag{1}$$

where ω is the angular frequency; k_z is the axial wave number; c is the speed of light in vacuum; R_0 is the waveguide radius; and $p_{l\nu}$ is the νth root of the lth order Bessel function of the first kind.

If the operating frequency of the device is greater than the plasma frequency ($\omega > \omega_p$), the electromagnetic waves in the plasma-loaded waveguide are very similar to the TM waves in a smooth-walled empty waveguide, as can be seen from (1). The only difference is that the cutoff frequency for the plasma-filled guide is increased relative to the empty waveguide by:

$$\omega_{co}^2 = \left(\frac{p_{l\nu}}{R_0}\right)^2 + \omega_p^2. \tag{2}$$

This shift in the cutoff frequency can be seen in Fig. 1(b), where the dispersion curve for the lowest-order symmetric electromagnetic mode (labeled "TM_{01}") is displayed. In addition, the presence of the plasma in the waveguide allows k_z^2 to take on positive real values for $\omega < \omega_p$, thus giving rise to a propagating wave. Fig. 1(b) also displays plots of several plasma-guide (T–G) modes. The geometry of the problem is shown in Fig. 1(a).

Thus the lower branches in Fig. 1(b) represent a family of plasma-guide modes having a high-frequency cutoff at ω_p and no low-frequency cutoff. One of the interesting features of the plasma-guide modes is that the high-frequency cutoff is independent of the geometry and depends only on the plasma frequency. This is in contrast with the electromagnetic waveguide modes whose cutoff frequencies depend intimately on the geometry. Another difference between the plasma-guide and electromagnetic modes is the fact that for operating frequencies within the plasma-guide mode band ($0 < \omega < \omega_p$), all of the plasma-guide modes ($l \geq 0$, $\nu \geq 1$) will propagate simultaneously if excited. In contrast, at frequencies above the plasma frequency the number of electromagnetic wave-

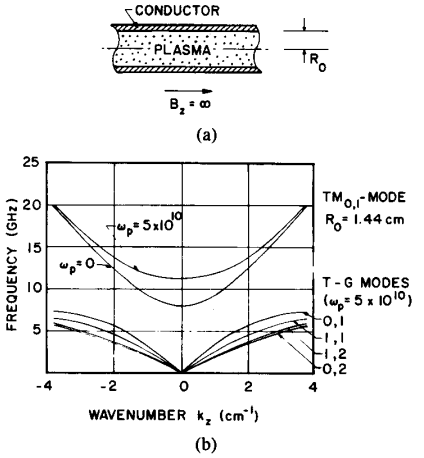

Fig. 1. (a) A smooth-wall plasma-loaded waveguide immersed in an infinitely large guiding magnetic field (model of Section II). (b) The dispersion relation for a plasma-loaded smooth-wall waveguide having a radius of $R_0 = 1.44$ cm. A single TM_{01} mode with and without a plasma, as well as several plasma-guide (T-G) modes, are shown.

guide modes that can propagate at any given frequency is finite, though increasing with frequency. The principal feature of plasma-guide propagation is that a plasma column can support modes of wave propagation below the plasma frequency, even in the absence of electron drift motion.

As was pointed out earlier, the plasma-guide modes are electromechanical in nature. The wave propagation results from the interchange between the kinetic energy of the electrons and the stored energy in the electric field. In contrast, for the case of electromagnetic waves in an evacuated waveguide, the wave propagation results from the interchange of the electric and magnetic stored energy. Nevertheless, there are some similarities between the two families of waves in terms of the field components, mode structure, and power-carrying capabilities. Table I compares the field components and power carried by the two classes of waves for the case of azimuthal symmetry ($l = 0$).

The two families of modes propagate in two different frequency ranges. While the T-G (plasma-guide) modes propogate below the plasma frequency, the electromagnetic modes can only propagate at frequencies above:

$$\omega > \left[\omega_p^2 + \left(\frac{p_{0\nu}}{R_0}\right)^2\right]^{1/2}. \tag{3}$$

Using Table I, a number of informative plots for the T-G modes may be generated. For example, Fig. 2 shows the electric field configuration for the two lowest-order T-G modes ($T\text{-}G_{(0,1)}$ and $T\text{-}G_{(0,2)}$). The power carried by these same modes as a function of frequency is plotted in Fig. 3, where a plasma frequency of 4 GHz and a maximum electric field amplitude of 100 kV/cm has been assumed. From this figure it is clear that the presence of the plasma inside the waveguide does not lower the power-handling capabilities of the system. As the wave frequency of the T-G mode approaches the plasma frequency, the wave becomes increasingly electrostatic in nature, its power-carrying capability diminishes, and its group velocity $\partial\omega/\partial k$ decreases to zero. Fig. 4 shows the radial distribution of the three field components E_z, E_r, and H_θ for the lowest order ($l = 0$, $\nu = 1$) symmetric plasma-guide mode for various frequencies. As before, as ω approaches $\omega_p = 4$ GHz (in this example), both H_θ and E_r decrease to zero. Only the electrostatic component E_z remains unchanged.

TABLE I
FIELD COMPONENTS AND AXIAL POWER FLOW FOR AZIMUTHALLY SYMMETRIC ELECTROMAGNETIC ($TM_{0\nu}$) AND PLASMA-GUIDE (T-G) MODES

	Symmetric $TM_{0,\nu}$ Mode in Empty Cylindrical Waveguide	Symmetric Plasmaguide (T-G) Mode in Cylindrical Waveguide
E_z	$A\,J_0(k_c r)$	$A\,J_0(k_c r)$
E_r	$-jA\frac{k}{k_c}J_0'(k_c r)$	$-jA\frac{k}{k_c}(1-\frac{\omega_p^2}{\omega^2})J_0'(k_c r)$
H_ϕ	$-jA\frac{\omega\epsilon}{k_c}J_0'(k_c r)$	$-jA\frac{\omega\epsilon}{k_c}(1-\frac{\omega_p^2}{\omega^2})J_0'(k_c r)$
Axial power flow, P	$\frac{1}{2}\pi R_0^2\lvert A\rvert^2\frac{k\omega\epsilon}{k_c^2}J_1^2(k_c r)$	$\frac{1}{2}\pi R_0^2\lvert A\rvert^2\frac{k\omega\epsilon}{k_c^2}(1-\frac{\omega_p^2}{\omega^2})^2 J_1^2(k_c r)$

$k_c = p_{0\nu}/R_0$: Cut-off wavenumber for the specific mode of interest. $A = E_z(r = 0)$: Electric field amplitudes on axis.

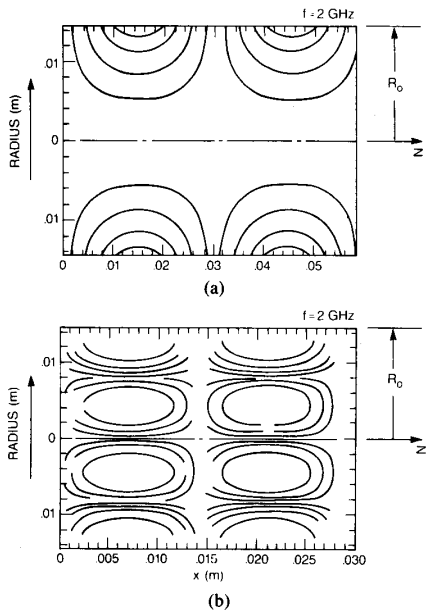

Fig. 2. Electric field configuration for the two lowest-order, symmetric-plasmaguide modes. (a) $T\text{-}G_{(0,1)}$. (b) $T\text{-}G_{(0,2)}$. Both were calculated for $\omega_p = 2\pi \cdot 4$ GHz, $R_0 = 1.44$ cm at a frequency of 2 GHz.

III. SPACE-CHARGE-LIMITING CURRENT IN PLASMA-LOADED WAVEGUIDES

In essence, a backward-wave oscillator consists of an electron beam confined radially by a strong longitudinal

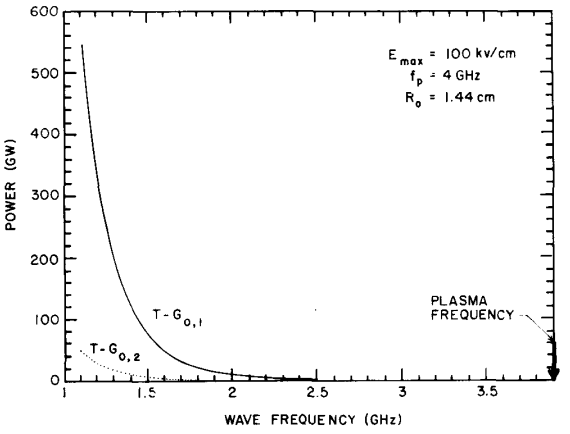

Fig. 3. Calculated power-carrying capabilities of the two lowest-order symmetric plasma-guide modes versus frequency ($\omega_p = 2\pi \cdot 4$ GHz).

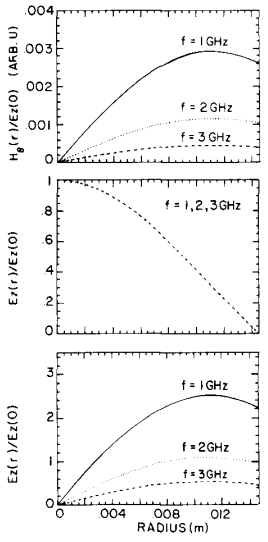

Fig. 4. Calculated radial dependence of E_z, E_r, and H_θ for the lowest-order, symmetric plasma-guide mode at few frequencies ($\omega_p = 2\pi \cdot 4$ GHz, $R_0 = 1.44$ cm).

magnetic field and propagating axially through a slow-wave structure. The slow-wave structure consists of a cylindrical waveguide with a periodically varying wall radius $R(z)$ sinusoidally rippled about the mean radius R_0, such that:

$$R(z) = R_0 + h \cos k_0 z \tag{4}$$

as shown in Fig. 5, where h is the ripple amplitude, z_0 is the ripple period, and $k_0 = 2\pi/z_0$.

The slow-wave structure supports a set of electromagnetic modes in the waveguide which has phase velocities parallel to the beam velocity and propagate at less than the speed of light. These slow electromagnetic waves interact resonantly with the negative energy slow space-charge wave supported by the beam, which leads to an instability that transfers kinetic energy from the beam to

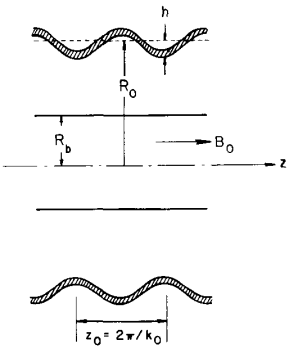

Fig. 5. The slow wave structure and beam model of Section III.

the electromagnetic field of the structure. The backward-wave oscillator is so named because, at the point of beam and electromagnetic structure-mode resonance, the structure mode has a negative group velocity, resulting in the propagation of electromagnetic energy backward along the beam—i.e., the Poynting vector points antiparallel to the beam velocity.

As indicated in Section I, recent theoretical studies have predicted that the introduction of a plasma into vacuum HPM devices may lead to greatly enhanced performance [2], [10]–[16]. For the purposes of the discussion of the space-charge-limiting current, we will approximate the corrugated-wall waveguide with a smooth-walled waveguide having the same average radius. In the presence of a background plasma, the space-charge-limiting current in a smooth-walled cylindrical waveguide can be increased by a factor of $(1 - f)^{-1}$, where $f = n_i/n_e$ represents the amount of charge neutralization provided by the ions in the background plasma. The increased space-charge-limiting current may allow microwave-generating devices to transport more intense electron beams, leading to the possibility of generating enhanced power levels.

The space-charge-limiting current in the presence of the plasma for a thin hollow beam with a mean radius R_b and a thickness $\Delta << R_b$ is given by [18]:

$$I_l = \frac{17[\gamma^{2/3} - 1]^{3/2}}{[2 \ln (R_0/R_b)][1 - f]} \text{ [kA]} \tag{5}$$

where $\gamma = (1 - v^2/c^2)^{-1/2}$ is the relativistic mass factor for the beam electrons. By increasing the beam current through introduction of a background plasma, a new limitation is encountered which is imposed by the onset of beam-plasma instability. This instability will occur at current levels that are larger than the vacuum-limiting current by the factor [2]:

$$\left[\frac{\gamma(1 - \gamma^{-2})}{(1 - \gamma^{-2/3})}\right]^{3/2}. \tag{6}$$

For mildly relativistic electron beams having $\gamma = 3$, the actual current carried by the beam in the presence of

plasma may be as much as seven times larger than the vacuum case. The increased injected current level may simply allow operation at higher beam power and result in enhanced microwave power output without affecting the interaction efficiency or the physical interaction mechanism.

IV. Linear Theory of Plasma-Loaded Corrugated Waveguides

In addition to affecting the space-charge-limiting current, the presence of plasma in the slow-wave structure may completely alter the nature of the beam–wave interaction, leading to greatly enhanced device power-generation efficiency. The studies reported here are the first that clearly belong to this latter category.

The linear theory of thin annular beams in an evacuated corrugated wall structure has been treated both analytically and numerically by researchers in the U.S. [19] and the Soviet Union [20]. The introduction of plasma into the slow-wave structure, however, necessitates the development of an extension to the vacuum theory. Previous treatment of the linear theory of plasma-loaded structures [21], [22] used the approximation of small corrugation amplitudes ($h/R_0 << 1$). Recently, a linear theory allowing for the treatment of arbitrarily large corrugation amplitudes has been developed. A complete description of the theory can be found in [23]. The main results of this linear theory describing the excitation of electromagnetic waves in a plasma-filled BWO by a relativistic electron beam are presented below, where the dispersion relation and growth rates of plasma-filled periodic structures have been calculated.

In developing the linear theory the following assumptions were made: (i) The magnitude of the axial-guiding magnetic field is taken to be infinite, confining the electron motion in the beam to one dimension; (ii) the beam is monoenergetic, with an axial streaming velocity v_b; (iii) the beam is of uniform density N_b and completely fills the waveguide; (iv) the waveguide is infinite in length and the waveguide wall is perfectly conducting; (v) only the symmetric ($TM_{0\nu}$) electromagnetic modes are considered; and (vi) the plasma-guide modes are neglected.

In general, the linearized normal electromagnetic modes of a periodic corrugated wall structure are the transverse electric (TE) modes, with electric and magnetic field components E_θ, B_r, and B_z, and the transverse magnetic (TM) modes, with field components E_r, E_z, and B_θ. In our idealized one-dimensional system the TE waves do not perturb the axial electron motion and will not be considered further, since they cannot cause beam instabilities. The TM waves, on the other hand, are capable of perturbing the axial beam velocity and beam density and assumption (v) above is justified.

The periodicity of the slow-wave structure permits the field components and beam perturbation to be expanded in an infinite Floquet sum. Assuming azimuthal symmetry, the axial and radial components of the $TM_{0\nu}$ electric field can be expressed as [23]:

$$E_z = \sum_{n=-\infty}^{\infty} A_n J_0\left(\frac{x_n}{R_0} r\right) \exp\left[i(k_n z - \omega t)\right] \tag{7}$$

$$E_r = \sum_{n=-\infty}^{\infty} A_n \left[-\frac{ik_n x_n}{R_0\left(\frac{\omega^2}{c^2} - k_n^2\right)}\right] J_1\left(\frac{x_n}{R_0} r\right) \cdot \exp\left[i(k_n z - \omega t)\right] \tag{8}$$

where ω_b is the beam-plasma frequency, and

$$k_n = k_z + nk_0$$

$$x_n^2 = R_0^2\left(\frac{\omega^2}{c^2} - k_n^2\right)\left[1 - \frac{\omega_p^2}{\omega^2} - \frac{\omega_b^2 \gamma^{-3}}{(\omega - k_n v)^2}\right].$$

Assumption (iv) requires that the tangential electric field vanishes at the waveguide wall. Using the axial and radial electric-field components of (7) and (8), we express this boundary condition in matrix form as:

$$\boldsymbol{D} \cdot \boldsymbol{A} = \sum_{m,n=-\infty}^{\infty} A_n D_{m,n} = 0 \tag{9}$$

where $\boldsymbol{A}$ is a column vector with elements A_n, and $\boldsymbol{D}$ is a matrix with elements $D_{m,n}$. A dispersion relation results when a nontrivial solution to (9) is found by solving the determinant equation $\det|\boldsymbol{D}| = 0$.

In order to numerically analyze experimental systems, the infinite matrix of (9) must be truncated to a finite size. For example, to analyze an experimental system with a corrugation amplitude ratio $h/R_0 = 0.3$, a truncated matrix with a rank of nine was found to be sufficient.

Fig. 6 displays the calculated TM_{01} mode dispersion curves in a plasma-filled corrugated waveguide for a variety of plasma densities. The beam space-charge line, assuming infinitesimal beam density ($\omega_b = 0$), is superimposed on this dispersion curve and has been plotted for the case which corresponds to the experimental parameters to be described in the next section. As can be seen in Fig. 6, the presence of the plasma tends to raise the TM_{01} mode cutoff frequency relative to the vacuum cutoff frequency while also causing a decrease in the group velocity everywhere, resulting in a "flattening" of the dispersion relation.

When the beam density is neglected ($\omega_b = 0$), the radiation frequency ω is real for real values of the axial wave number k_z and no instabilities are expected. To obtain the TM_{01} growth rates, a nonzero value of ω_b must be used and the dispersion equation must be solved for complex values of ω for real values of k_z. Fig. 7 displays the growth rate $\mathrm{Im}(\omega/2\pi)$ calculated for the experimental parameters. The results are similar to those found in [15], with the exception that in this case the peak growth rate is a function of the plasma density as shown in Fig. 8. The calculations predict, therefore, a considerable decrease in the linear growth rate for plasma densities of $N_p \geq 10^{12}$ cm^{-3}.

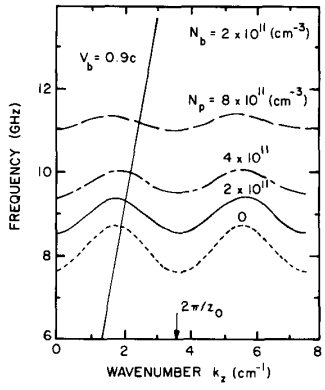

Fig. 6. The calculated effect of varying the plasma density on the corrugated waveguide dispersion ($R_0 = 1.445$ cm, $h = 0.445$ cm, $z_0 = 1.67$ cm).

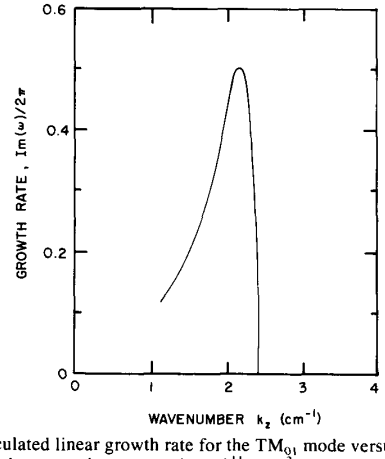

Fig. 7. Calculated linear growth rate for the TM_{01} mode versus wavenumber k_z for the case where $N_p = 2 \cdot 10^{11}$ cm^{-3}, $N_b = 6.3 \cdot 10^{10}$ cm^{-3} (solid beam).

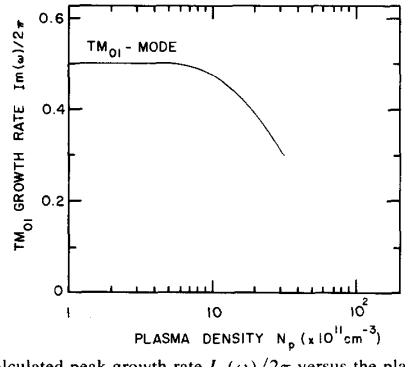

Fig. 8. Calculated peak growth rate $I_m(\omega)/2\pi$ versus the plasma density for the TM_{01} mode (solid beam of density $N_b = 6.3 \cdot 10^{10}$ cm^{-3}).

V. Measurement of Efficiency in a Plasma-Loaded BWO

Early experiments testing the effect of plasma on the operation of vacuum BWO's utilized background plasmas produced by electron-beam impact ionization of a low-pressure neutral background gas to demonstrate enhanced microwave output power [7], [8]. In recent experiments [9] an independently controllable Argon plasma source was used to inject plasma directly into the BWO slow-wave structure, as shown in Fig. 9.

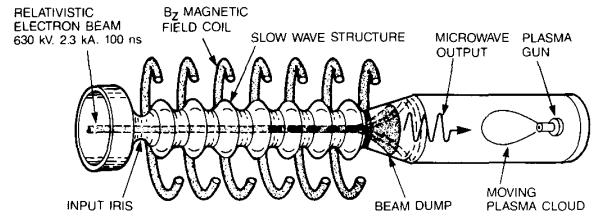

Fig. 9. Schematic diagram of the plasma-loaded BWO experiment. The electron beam is injected from the left and the radiation is extracted at right, where the plasma is injected.

A hollow relativistic electron beam with an injection energy of 630 keV, a beam current of 2.3 kA, and a pulse duration of 100 ns (Fig. 10) was propagated in a sinusoidally rippled slow-wave structure immersed in a uniform axial magnetic field of ~ 12 kG. The slow-wave structure had an average radius $R_0 = 1.445$ cm, a corrugation amplitude $h = 0.44$ cm, a corrugation period of $z_0 = 1.67$ cm, and a structure length of 8 periods. The electron beam had an average radius of 0.8 cm, a thickness of 0.2 cm, and an electron density of $\sim 5 \times 10^{11}$ cm^{-3}.

A coaxial plasma gun [24] was located approximately 100-cm downstream of the slow-wave structure in a field free region and generated an Argon plasmoid which crossed the magnetic field lines at an average velocity of about 1.2 cm/μs on its way towards the interaction region. The system was pre-evacuated to a pressure of $< 4 \times 10^{-5}$ T.

In separate experiments the plasma column density was measured with both a 35- and 70-GHz microwave interferometer and its velocity, density, and temperature was measured with Langmuir probes. Preliminary results indicate that the average plasma density could be varied by changing the plasma gun voltage and gas pressure. Realizable plasma densities in the slow-wave structure ranged from 0 up to a maximum value estimated at $\sim 10^{12}$ cm^{-3}.

There were three principal overlapping time scales in the BWO experiments: The longest time scale was on the order of 10 ms, corresponding to the quarter-cycle time of the pulsed axial-guiding magnetic field. The second longest time scale was on the order of 100 μs, corresponding to the plasma generation and propagation time from the plasma gun to the slow-wave structure. Finally, as noted above, the beam pulse duration was 100 ns. The three time scales were all synchronized such that the beam and plasma interacted in the slow-wave structure during the time that the applied magnetic field was nearly constant and at its peak value.

The plasma density in the slow-wave structure was intentionally varied from shot-to-shot in order to determine its effect on the operational efficiency of the BWO. The plasma density was varied in the slow-wave structure by delaying the time of beam injection into the slow-wave

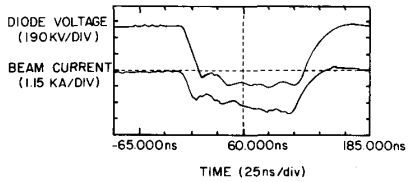

Fig. 10. Diode voltage (top trace) and BWO beam-current waveforms used in the experiment. An annular beam with an average radius of 0.8 cm and a thickness of 0.2 cm was used.

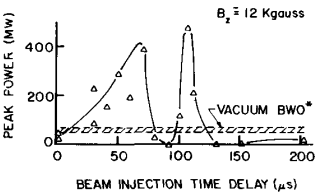

Fig. 11. Peak microwave power (at 8.4 GHz) versus the beam-injection time delay. By adjusting this delay we can set the desired plasma density in the BWO before the injection of the electron beam.

structure relative to the time of initial plasma generation. By changing the relative delay times from shot-to-shot, a greater or lesser density plasma was allowed to diffuse into the slow wave structure at the instant of beam injection.

An enhancement of the microwave power-generation efficiency was observed over a wide range of injected plasma densities, $0 < N_p < N_{p(cr)}$, where $N_{p(cr)}$ is a critical plasma density. This critical plasma density, to be discussed in Section VII, occurred at a delay time $\Delta t \sim 90$ μs relative to the initial generation of the plasma. The efficiency enhancement factor over vacuum BWO operation was found to be dependent on the plasma density and reached a maximum value of eight when the electron beam was injected into an optimized plasma density.

The points of maximum BWO efficiency enhancement were found to occur for two different time delays—once for a short time delay $\Delta t \sim 60$ μs, which occurred during the plasma buildup in the slow-wave structure, and then again for a longer delay $\Delta t \sim 100$ μs, which occurred during the plasma decay. Fig. 11 is a plot of the peak radiated power (at 8.4 GHz) as a function of the beam-injection time delay Δt gathered over a number of shots. At the points of maximum enhancement, indicated by the two relative maxima of Fig. 11, the interaction efficiency increased to almost 40%, compared with approximately 5% for a vacuum BWO under the same operating conditions. The output power was measured using a side coupler calibrated for the TM_{01} mode over the relevant bandwidth.

The plasma density in the slow-wave structure reached its highest values for beam-injection time delays in the range 60 μs $< \Delta t <$ 100 μs. In this range the BWO radiation at 8.4 GHz from the fundamental TM_{01} mode was quenched and higher frequency emission in the 12–18-GHz range was observed. At these higher plasma densities the BWO was considered to be overdriven and switched from the fundamental TM_{01} mode to TM_{02} and possibly higher order modes, as indicated in Fig. 12.

An example of the change in frequency spectra that accompanies mode switching is shown in Fig. 13, which plots the single-shot experimental spectrum for an efficiency-enhanced BWO, shown in Fig. 13(a), and an overdriven BWO, as shown in Fig. 13(b). These experimental curves were obtained using a dispersive line technique, where different frequency components are resolved by their different propagation velocities in a dispersive waveguide. Fig. 13(a) plots the power spectrum emitted by the BWO under the condition of strong plasma enhancement, where the dominant frequency component is centered near 8.4 GHz. A timing-reference microwave signal (labeled prompt) is superimposed on the dispersed signal. Fig. 13(b) represents the spectrum for an overdriven device in which mode switching has clearly occurred and frequency components in the range of 12–18 Gz are present, corresponding to TM_{02} or higher order modes as well as plasma oscillation. At even higher plasma densities microwave breakdown within the device will occur.

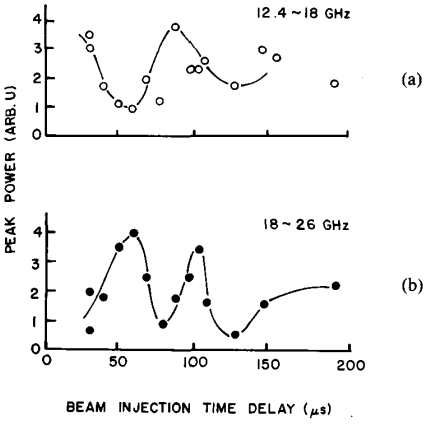

Fig. 12. Microwave radiation detected from the plasma-loaded BWO in the frequency bands: (a) 12–18 GHz (corresponding to emission at high-order mode); and (b) 18–26 GHz (which may correspond to emission due to an electromagnetically pumped FEL; see discussion).

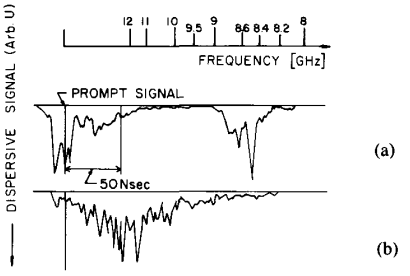

Fig. 13. Spectral results from plasma-enhanced backward-wave oscillator. (a) Maximum enhancement; and (b) overdriven device. The "prompt signal" is a timing reference.

Strong microwave emission was also detected in the 18–26 GHz band, proportional in amplitude to the fun-

damental TM_{01} backward-wave oscillations. These high frequencies are believed to be produced by a free-electron laser interaction driven by an electromagnetic pump, as previously reported [25], [26].

In our experiments the introduction of plasma into the device had no adverse effects on the diode voltage and current. The beam current entering the slow-wave structure was unaffected by the presence of the plasma and no effect on the diode shorting time was observed.

VI. Discussion of Results, Coupling Mechanisms, and Future Trends in Plasma Microwave Electronics

As the experiments described in the previous section demonstrate, the presence of a controlled plasma in the BWO slow-wave structure strongly enhances the interaction efficiency over a very wide range of plasma densities. In addition to efficiency enhancement, two other interesting features of the experimental results are: BWO plasma-saturation effects, and mode switching.

It was anticipated that overdriving the device with plasma above a critical density $N_{p(cr)}$ would lead to a quenching of the BWO interaction. As discussed in Section IV, the presence of plasma in the slow-wave structure tends to raise the lower cutoff frequency while simultaneously causing a flattening of the overall dispersion curves. If the device is overdriven to a point where the lower and upper cutoff frequencies are similar, the electromagnetic-mode group velocity is drastically reduced and no backward wave interaction is possible.

The linear theory of electromagnetic waves in plasma-loaded BWO's, presented in Section III, predicts that BWO TM_{01} quenching by plasma saturation might be observed for critical densities,

$$N_{p(cr)} \cong 10^{12}[\mathrm{cm}^{-3}]. \tag{10}$$

If the plasma density is above this critical value, the linear growth rate will begin to decrease as shown in Fig. 8. Linear theory also predicts that mode switching may occur at about the same critical density [23]. Indeed, both BWO plasma saturation, as seen in Fig. 11, and mode switching, as seen in Figs. 12 and 13, were observed when the device was overdriven. This occurred when the beam-injection delay time was adjusted to $\Delta t \sim 90\ \mu$s, corresponding to an estimated plasma density of $N_p < 2 \times 10^{11}$ cm^{-3}, which is far below the value predicted by the linear theory.

The linear theory for a plasma-loaded fundamental TM_{01} mode in a BWO predicts that the interaction frequency of the BWO will increase with increased plasma density, as may be seen in Fig. 6. This predicted increase has not yet been observed experimentally. Recent data indicates that the radiation frequency remains fixed (within the measurement resolution) despite changes in the plasma density. The growth rate predicted by the theory is only slightly larger in the presence of the plasma as compared to the vacuum BWO case.

Thus while the linear theory is successful at predicting some experimentally observed trends such as reduction of the growth rate (plasma saturation) and mode switching due to the presence of the plasma, it does not produce numerical results that are reasonably close to the experimental data. This leads us to the conclusion that the present linear theory must be extended to account for the observed experimental results.

One physical mechanism which may explain the enhanced efficiency is a three-wave interaction involving the beam, electromagnetic, and T-G plasma waves in the periodic slow-wave structure. In a nonperiodic structure, the normal T-G modes will not interact with a relativistic electron beam, as their phase velocities are small compared to the phase velocity of the beam space-charge wave. In a periodic structure, however, the T-G modes are also expected to exhibit periodicity in k-space, as required by the Floquet theorem. The dispersion curve for a periodic plasma is quite different from that shown in Fig. 1(b) for a plasma in a smooth-walled waveguide. Most significantly, there exist some periodic T-G modes that have phase velocities that are equal to that of the relativistic electron beam and are capable of supporting backward waves.

As an example, Fig. 14 plots the uncoupled, shifted dispersion curves for the $T\text{-}G_{(0,2)}$ modes (labeled as "plasma waves"), and also the approximate coupled dispersion relation for this mode. The dispersion curve for the lowest-order electromagnetic mode (labeled "TM_{01}") can also be seen. Azimuthal symmetry has been assumed, and, for clarity, only the first five periods in k have been plotted.

For the range of values of the plasma density and beam energy relevant to the experiments reported in this paper, the beam is simultaneously in synchronism with the backward branch of the electromagnetic structure wave and several backward branches of the periodic plasma waves. The slow space-charge wave and the lowest order TM_{01} electromagnetic wave have the same phase velocity ω/k as do one or more of the periodic T-G waves. In addition, the three waves all share a strong common component of the axial electric field E_z. It is possible that the enhanced efficiency observed in the experiment results from this three-wave synchronism; namely, induced scattering of the electromagnetic radiation of electrons in an electrostatic field produced by the background plasma in the presence of a periodic, perfectly conducting wall.

An efficient three-wave interaction also implies a very broad gain curve with respect to the electron-beam energy. This implication is consistent with the foregoing proposed mechanism, since the beam electrons tend to stay in synchronism with both of the backward branches, even as the beam is losing energy. A change of 40% in the beam kinetic energy corresponds to a change of less than 5% in the streaming velocity for our experimental conditions.

A second mechanism which may explain the enhanced emission in the presence of the plasma is a stimulated Raman scattering process which may be described using a

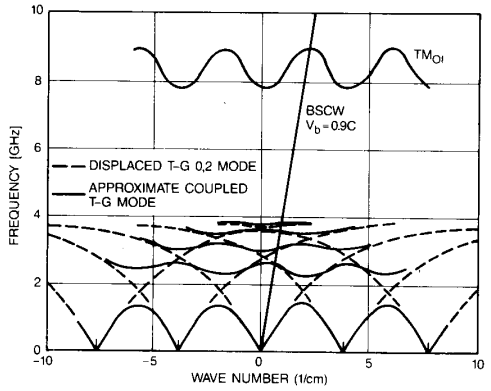

Fig. 14. Schematic sketch of the dispersion diagram for the electromagnetic TM_{01} mode, the plasma-guide $T\text{-}G_{(0,2)}$ mode, and a space-charge wave on a low-density beam traveling at $v_b = 0.9c$ (see discussion).

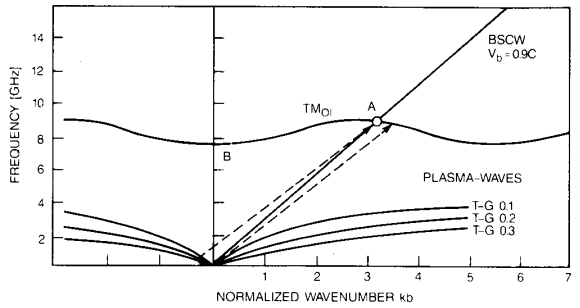

Fig. 15. Schematic sketch of Stokes diagram for three-wave interaction, which involves a backward branch of the plasma-guide (T-G) mode, and two TM_{01} waves of somewhat different frequencies.

Stokes diagram, as shown in Fig. 15. In this figure, the electromagnetic wave (point A) decays into a backward plasma-guide (T-G) wave and an electromagnetic wave which is slightly shifted in frequency. Thus this mechanism proposes a multiwave interaction as the explanation for enhanced efficiency.

It should be noted that for the experiments described in this work, the electron-beam current was always below that of the vacuum limit for the device geometry. As a result, we have not yet studied the radiation generation mechanism at beam currents above this limit. As discussed in Section III, the introduction of plasma into the slow-wave structure may have the effect of neutralizing the RF space charge in the beam (allowing a greater degree of axial bunching) and also may allow the propagation of beam currents above the vacuum space-charge limit. This phenomenon is of great interest to the field of relativistic microwave electronics and may be the subject of future experimental work.

It is anticipated that plasma injection may also prove beneficial to a variety of high-power microwave devices [12]–[16], [21]. Gyrotrons, for example, may achieve a greater degree of tunability and yield higher output power by overcoming the space-charge limit [14].

It was predicted theoretically [12] that larger gain can be realized in plasma-loaded free-electron lasers that are expected to exhibit greater tunability and performance enhancement by changing the refractive index n in the cavity [13].

Acknowledgment

The authors would like to acknowledge the helpful discussions with Drs. T. Antonsen, Jr., J. Booske, B. Levush, A. Ron, and V. K. Tripathi and the technical assistance of D. Cohen and J. Pyle.

References

[1] D. Bohm and E. Gross, "Plasma oscillations as a cause of acceleration of cosmic ray particles," *Phys. Rev.*, vol. 74, no. 5, p. 624, Sept. 1948.
I. Akhiezer and Ya. B. Fainberg, *Dokl. Akad. Nauk. SSSR*, vol. 65, p. 555, 1949.

[2] M. V. Kuzelev *et al.*, "Relativistic high-current plasma microwave electronics: Advantages, progress and outlook," *Sov. J. Plasma Phys.*, vol. 13, no. 11, pp. 793–800, Nov. 1987.

[3] Special issues on high-power microwave generation, *IEEE Trans. Plasma Sci.*, vol. 13, Dec. 1985, and *IEEE Trans. Plasma Sci.*, vol. 16, Apr. 1988.

[4] S. P. Bugaev *et al.*, "Atmospheric microwave discharge and study of the coherence of radiation from a multiwave Čerenkov generator," *Sov. Phys.—Dokl.*, vol. 32, no. 1, pp. 78–79, Jan. 1988.

[5] S. P. Bugaev *et al.*, "Investigation of a millimeter wavelength range gigawatt power level multiwave Čerenkov generator," in *Proc. 7th Int. Conf. High-Power Electron Beams* (Karlsruhe, FDR), July 1988, vol. 1, pp. 454–460.
S. P. Bugaev *et al.*, "Investigation of a millimeter wavelength range relativistic diffraction generator," *IEEE Trans. Plasma Sci.*, this issue, pp. 518–524.

[6] V. I. Bratman *et al.*, "Relativistic Čerenkov source for the millimeter range," *Sov. Tech. Phys. Lett.*, vol. 9, no. 5, pp. 266–267, May 1983.

[7] Yu. V. Tkach *et al.*, "Emission by a relativistic beam at a magneto-Čerenkov resonance in a periodic waveguide," *Sov. J. Plasma Phys.*, vol. 5, no. 5, pp. 568–570, Sept.–Oct. 1979.

[8] K. Minami *et al.*, "Observation of resonant enhancement of microwave radiation from a gas-filled backward wave oscillator," *Appl. Phys. Lett.*, vol. 53, no. 7, pp. 559–561, Aug. 1988.

[9] Y. Carmel *et al.*, "Demonstration of efficiency enhancement in a high power backward wave oscillator by plasma injection," *Phys. Rev. Lett.*, vol. 62, no. 20, pp. 2389–2392, May 1989.

[10] L. S. Bogdankevich *et al.*, "Theory of excitation of plasma filled rippled boundary resonators by relativistic electron beams," *Sov. Phys.—Tech. Phys.*, vol. 25, no. 2, pp. 143–147, Feb. 1980.

[11] V. I. Kurilko *et al.*, "Effect of plasma on the amplification of regular waves by a relativistic beam in a corrugated waveguide," *Sov. Phys.—Tech. Phys.*, vol. 26, no. 7, pp. 812–815, July 1981.

[12] W. B. Pei and Y. S. Chen, "The effect of background plasma in the undulator on free electron lasers," *Int. J. Electron.*, vol. 65, no. 3, pp. 551–564, 1988.

[13] M. B. Reid *et al.*, "Novel approaches to FEL operation: The gas-loaded FEL and a high efficiency FEL design," *Int. J. Electron.*, vol. 65, no. 3, pp. 533–550, 1988.

[14] W. M. Manheimer *et al.*, "Experimental investigation of plasma neutralized operation of a gyrotron," *Bull. Amer. Phys. Soc.*, vol. 33, no. 9, p. 1956, Oct. 1988.

[15] J. S. DeGroot *et al.*, "High power and superpower plasma Čerenkov masers," in *Microwave and Particle Beam Sources and Directed Energy Concepts* (SPIE vol. 1061). SPIE, Jan. 1989.

[16] R. W. Schumacher *et al.*, "Millimeter wave generation via plasma three wave mixing," Hughes Res. Lab., Malibu, CA, Rep. No. F49620-85-C-0059.

[17] A. W. Trivelpiece and R. W. Gould, "Space charge waves in cylindrical columns," *J. Appl. Phys.*, vol. 30, no. 11, pp. 1784–1793, Nov. 1959.

[18] R. B. Miller, *Intense Charged Particle Beams*. New York: Plenum, 1982, p. 85.

[19] J. A. Swegle *et al.*, "Backward wave oscillators with rippled wall

resonators: Analytic theory and numerical simulation," *Phys. Fluids*, vol. 28, no. 9, pp. 2882-2894, Sept. 1985.
[20] V. I. Kurilko *et al.*, "Stability of a relativistic electron beam in a periodic cylindrical waveguide," *Sov. Phys.—Tech. Phys.*, vol. 24, no. 12, pp. 1451-1454, Dec. 1979.
[21] L. S. Bogdankevich *et al.*, "Theory of excitation of plasma filled rippled boundary resonators by relativistic electron beams," *Sov. Phys.—Tech. Phys.*, vol. 25, no. 2, pp. 143-147, Feb. 1980.
[22] V. I. Kurilko *et al.*, "Effect of a plasma on the amplification of regular waves by a relativistic electron in a corrugated waveguide," *Sov. Phys.—Tech. Phys.*, vol. 26, no. 7, pp. 812-815, July 1981.
[23] K. Minami *et al.*, "Linear theory of electromagnetic wave generation in a plasma-loaded corrugated wall resonator," *IEEE Trans. Plasma Sci.*, this issue, pp. 537-545.
[24] J. Marshall *et al.*, in *Proc. 2nd Int. Conf. Plasma Phys. Controlled Nucl. Fusion Res.* (Culham, UK), 1965. Vienna: IAEA, 1966, vol. 2, p. 449.
[25] P. G. Zhukov *et al.*, in *Proc. 3rd Int. Topical Conf. High Power Electron and Ion Beam Res. Tech.*, A. N. Skrinsky, Ed. Novosibirsk, USSR: Inst. Nucl. Phys., 1979, vol. 1, p. 705.
G. G. Denisov *et al.*, *Int. J. Infrared Millimeter Waves*, vol. 5, p. 1389, 1984.
[26] R. A. Kehs *et al.*, "Experimental demonstration of an electromagnetically pumped free electron laser with a cyclotron-harmonic idler," *Phys. Rev. Lett.*, vol. 60, no. 4, pp. 279-281, Jan. 1988.
R. A. Kehs *et al.*, "Free electron laser pumped by a powerful traveling electromagnetic wave," *IEEE Trans. Plasma Sci.*, this issue, pp. 437-446.

*

Yuval Carmel (S'66-M'74) was born in Israel in 1942. He received the B.Sc.(EE) and M.Sc.(EE) degrees from the Technion, Israel Institute of Technology, in 1966 and 1971, respectively, and Ph.D.(EE) degree from Cornell University, Ithaca, NY, in 1974.

He was with the Government of Israel, the Naval Research Laboratory, and is currently with the University of Maryland, College Park. His research interests include electromagnetic radiation from intense electron beams, free electron lasers, advanced concepts in millimeter-wave tubes, gyrotrons, and backward wave oscillators.

*

K. Minami, photograph and biography not available at the time of publication.

*

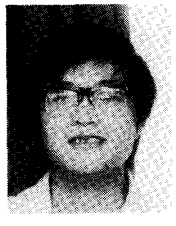

Weiran Lou was born in Hangzhou, China, on July 2, 1963. He received the B.S. (electrical engineering, 1983) and M.S. (optical engineering, 1986) degrees from Zhejiang University, Hangzhou, China. He is currently a Ph.D. degree candidate in the Electrical Engineering Department, University of Maryland, College Park. His research interests include high-power microwave generations and microwave-plasma interaction.

R. Alan Kehs (S'68-M'75-SM'88) received the B.S. and M.S. degrees in electrical engineering, and the M.S. and Ph.D. degrees in physics from the University of Maryland, College Park, in 1970, 1973, 1984, and 1987, respectively.

He has been employed by the Harry Diamond Laboratories, Adelphi, MD, since 1975, where his research interests have centered on the generation and use of intense relativistic electron beams—with emphasis on the production of high-power microwave radiation.

Dr. Kehs is a member of Eta Kappa Nu, Sigma Xi, and the American Physical Society.

*

William W. Destler (M'84), photograph and biography not available at the time of publication.

*

Victor L. Granatstein (S'59-M'64-SM'86) received the Ph.D. degree in 1963 from Columbia University, New York City, in electrical engineering and plasma physics.

After a year of postdoctoral work at Columbia University, he was a member of the Technical Staff of Bell Telephone Laboratories from 1964-1972. During 1969-1970 he was a Visiting Senior Lecturer at the Hebrew University of Jerusalem. In 1972 he joined the Naval Research Laboratory as a Research Physicist and from 1978-1983 served as Head of the High-Power Electromagnetic Radiation Branch. In August 1983 he became a Professor in the Electrical Engineering Department at the University of Maryland, College Park, and also serves as a Consultant to the Naval Research Laboratory, the Science Applications International Corporation, the Jet Propulsion Laboratory, and the State of Maryland (Department of Natural Resources). He is presently leading experimental and theoretical studies of electromagnetic radiation from relativistic electron beams, advanced concepts in millimeter-wave tubes, free electron lasers, and gyrotron amplifiers. He is Associate Editor of the *International Journal of Electronics* and has been a Guest Editor of the IEEE TRANSACTIONS ON MICROWAVE THEORY AND TECHNIQUES and the IEEE JOURNAL OF QUANTUM ELECTRONICS. He has been a reviewer for the NSF, AFOSR, DOE DNA, ONR, and ARO. He has co-authored more than 100 research papers in regular journals, and holds a number of patents on active and passive microwave devices. Since 1988 he has been Director of the Laboratory for Plasma Research at the University of Maryland.

Professor Granatstein is a Fellow of the American Physical Society.

*

D. K. Abe, photograph and biography not available at the time of publication.

*

J. Rodgers, photograph and biography not available at the time of publication.